

R-545

**INFORMATION PROCESSING AND
DATA COMPRESSION FOR
EXOBIOLGY MISSIONS**

by

Louis L. Sutro

Revised June 1966

GPO PRICE \$ _____

CESTI PRICE(S) \$ _____

Hard copy (HC) 2.00

Microfiche (MF) .50

650 July 65

**INSTRUMENTATION
LABORATORY** ●

MASSACHUSETTS INSTITUTE OF TECHNOLOGY

Cambridge 39. Mass.

FACILITY FORM 602

N66 35777

(ACCESSION NUMBER)

41
(PAGES)

DR-7756-4
(NASA CR OR TMX OR AD NUMBER)

(THRU)

1
(CODE)

CS
(CATEGORY)

R-545

**INFORMATION PROCESSING AND
DATA COMPRESSION FOR
EXO BIOLOGY MISSIONS**

by

Louis L. Sutro

Revised June 1966


A report of work performed from
October 1965 through March 1966
under NASA Contract Number
NSR-22-009-138.

Presented at the 12th Annual Meeting
of the American Astronautical Society,
Disneyland Hotel Convention Center,
Anaheim, California, May 23-25, 1966

**INSTRUMENTATION LABORATORY
MASSACHUSETTS INSTITUTE OF TECHNOLOGY
CAMBRIDGE, MASSACHUSETTS**

*Prepared for publication by Jackson & Moreland
Division of United Engineers and Constructors, Inc.*

Approved


Associate Director

Approved


Deputy Director

ACKNOWLEDGEMENT

This report was prepared under the auspices of DSR Project 55-257, sponsored by the Biosciences Division of the National Aeronautics and Space Administration through Contract Number NSR-22-009-138.

Publication of this report does not constitute approval by NASA of the findings or conclusions contained herein. It is published for the exchange and stimulation of ideas.

Biological help was provided by Jerome Y. Lettvin and Warren S. McCulloch, engineering help by William Kilmer, Roberto Moreno-Diaz, Jerome Krasner and Richard Catchpole.

ABSTRACT

N66-35777

Techniques being developed for missions to Mars are part of a larger effort to develop a robot capable of carrying out programs and of self-programming within certain limits. Three development efforts at the Instrumentation Laboratory lead in this direction: Design of a layered processor like that in a frog's retina shows how a model of animal vision may reduce data for transmission to Earth and permit response to the environment. Design of a stereoscopic system suggests how a pair of layered processors, when fed data from two television cameras, may find the positions of objects. Design of a decision and control system like that of animals suggests how a system of this kind may decide in what direction a Mars lander should move, when it should perform each experiment and what it should report.

Author

TABLE OF CONTENTS

<u>Section</u>		<u>Page</u>
1	INTRODUCTION.	1
2	THE LAYERED PROCESSING OF A VISUAL SYSTEM.	2
	2.1 The Structure of a Visual System	2
	2.2 Properties of a Visual System	2
	2.3 Design of the Model (Ref. 5)	5
	2.4 Computation in Levels 1 and 2(a)*	9
	2.5 Computation in Level 2(a)	10
	2.6 Computation in Level 3	12
	2.7 Instrumentation with Available Components . . .	13
	2.8 Instrumentation with Integrated Circuits	15
	2.9 Application to Missions to Mars	15
3	STEREOSCOPIC SYSTEMS	16
	3.1 Why Stereoscopic?	16
	3.2 Camera-Counter Chain C	17
	3.3 Camera-Computer Chain D	18
	3.4 Application to Missions to Mars	19
4	DECISION AND CONTROL PROCESSORS	21
	4.1 General	21
	4.2 Reticular Formation	21
	4.3 Model of RF*	25
	4.4 Visual-Center	28
	4.5 Application of RF* to Missions to Mars	29
5	THE NEED TO CARRY KNOWLEDGE ALONG . . .	30
	LIST OF REFERENCES	31

INFORMATION PROCESSING AND DATA COMPRESSION FOR EXO BIOLOGY MISSIONS

1. INTRODUCTION

In designing interplanetary probes such as that we plan to put on Mars we are faced with the problem of exploring after the vehicle has landed. We are attempting to devise a self-moving probe capable of exercising judgments in a certain sense and handling a variety of contingencies. It would broadcast the results of its experiments rather than be a simple extension of our senses and movements into the alien world.

It is clear that technology supplies us increasingly reliable parts ever smaller and able to work on little power so that computers become more and more compact. At the same time the art of using these devices expands greatly so that they have ceased to be the novelties for study and have become, instead, common tools. A number of workers, concerned with this art (including us), are attempting to make a true robot, capable of self-programming within certain limits, one that is capable of handling a large sequence of choices, correcting itself when it makes an error in judgment. That is not to say that we are so rash as to claim that we can build an animal or an animal intelligence, but it would be intelligence of a sort, and one that would permit communication with us.

Each experiment proposed for Mars requires both a sensor system, designed for the problem, and a data processing system designed to bridge the gap between the sensor system and the way our minds work. We propose to subject the data of the experiments to a decision system similar to ours. What comes out of this robot must then comply with our criteria of interest and intelligibility.

Can this be done in time for a Mars landing in the 1970's? The only way to find out is to try.

This paper describes three development programs under way at the Instrumentation Laboratory. One is the design of the layered processing of a visual system. The second is the design of a stereoscopic system. The third is a decision and control system.

How would a robot reduce data? We propose that the robot carry with it measures of the usefulness to man of the data it acquires, so that it will send back only data which satisfies those measures. For each of the development programs to be described such measures will be suggested. But a more useful set of measures will have to come from you.

2. THE LAYERED PROCESSING OF A VISUAL SYSTEM

2.1 The Structure of a Visual System

Dr. Warren McCulloch refers to an eye as a "layered computer". By this he means that all the bipolar cells process the data they receive from the photoreceptor layer, passing it along to the ganglion cell layer. The latter processes the output of the bipolar-cell layer passing along the results of its computation to the layered structures of the brain.

We want to model the human visual system, but it comprises far more cerebral layers than we can model now. For that reason we sought an animal with fewer layers in its visual system but equal or greater complexity per layer. We found this in the visual system of the frog.

2.2 Properties of a Frog's Visual System

The species studied, the common leopard frog or *Rana pipiens*, responds to one color and to four pattern aspects of objects: edges, dark convex moving edge (bug), any time varying visual event, and dimming.

The retina of the frog has three layers of nerve cells: photoreceptors, bipolar cells, and ganglion cells, as shown schematically in Fig. 1. Each cell type is uniformly distributed over the retina.

The photoreceptor layer consists of several types of rods and cones. An individual photoreceptor apparently may have two output parameters. The first appears to be a logarithmic function of illumination, related to

the bleaching rate of a pigment. A second parameter appears to be a function of the history of illumination, related to the amount of bleached pigment.

Bipolar cells are so called because their two ends are somewhat alike. Horizontal cells make interconnections among bipolar cells in the layer of photoreceptor outputs. There are interconnections formed by amacrine cells in the layers of connections between bipolars and ganglion cells.

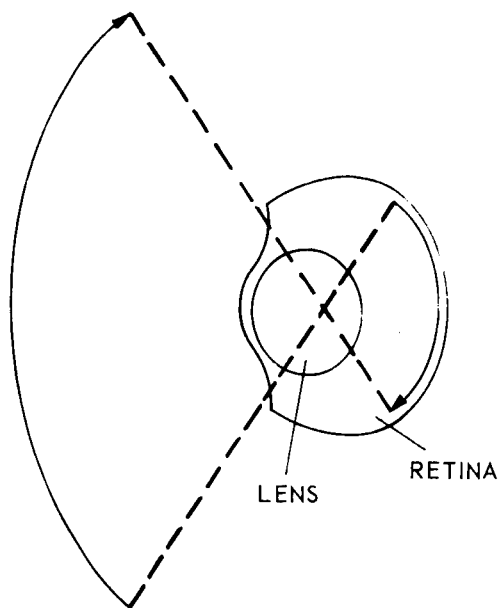
Ganglion cells appear to have five distinguishable dendritic arbors, that is, tree-like branchings. Three of these arbors are shown as O, P, and Q in Fig. 2. On the basis of the connections of bipolar cells to these arbors, Lettvin et al. were able to assign one of five functions to each arbor form;^(1, 2, 3) four concerning the visual pattern and one concerning color. The four pattern outputs go to the tectum (Fig. 1 right) while the color output goes to the geniculate body (not shown). The first four cell groups produce outputs representing:

1. Edge detection
2. Bug detection
3. Event detection (any stimulus change)
4. Dimming detection.

Of the approximately 5×10^5 ganglion cells (Fig. 1) approximately half are bug detectors. Since this has proved to be the most difficult ganglion cell to model,^(4,5) we have concentrated on it.

Figure 3 portrays vertical sections of two bipolar cells and one multi-level E-shaped ganglion cell, as drawn by Ramon y Cajal for the frog.⁽⁶⁾ In the latter there are three dendritic levels. Lettvin et al identified this structure as a bug detector. Note that arborization exists between the two outer dendritic levels.

Two types of bipolar cells will be represented in the model. Their designation "on" and "off", is that of Schwyperheyn.⁽⁷⁾ The distinction between "on" and "off" cells was previously applied by Hartline to ganglion cells.⁽⁸⁾



SECTION THROUGH FROG'S EYE ACCORDING TO CAJAL.

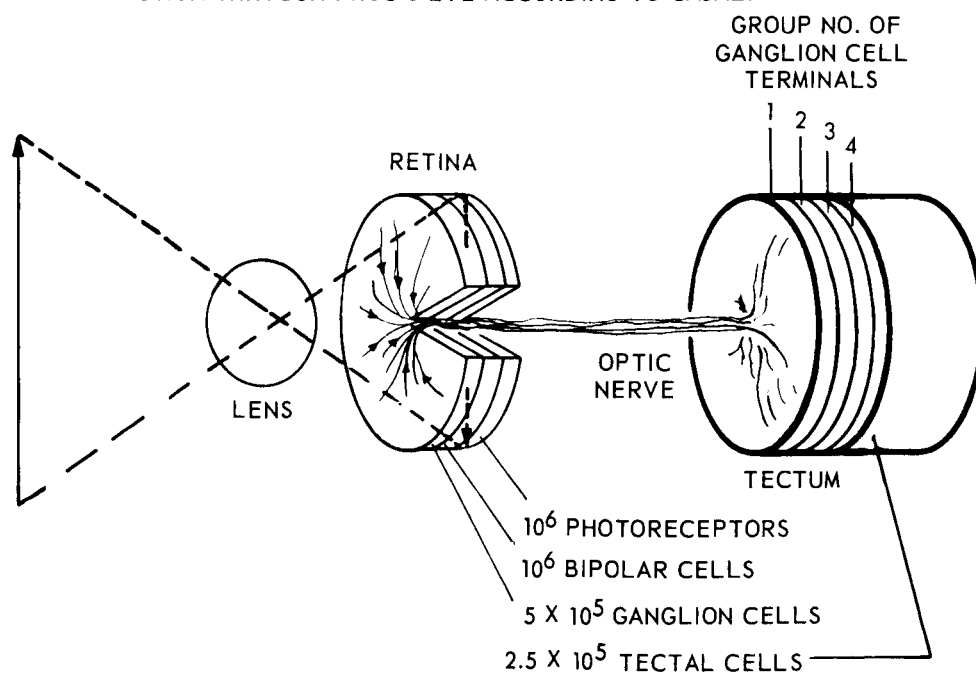


Fig. 1. Schematic of frog visual system.

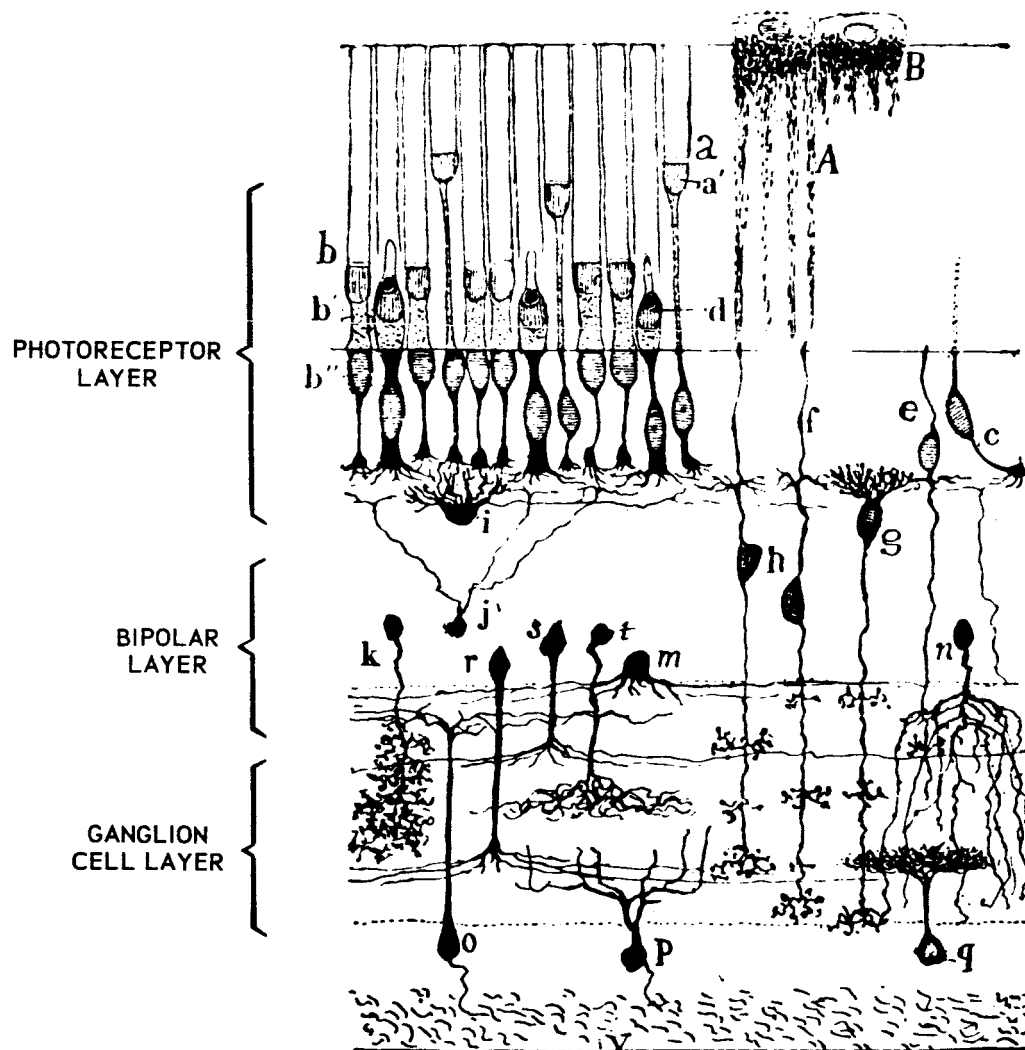


Fig. 2. The retina of frog in Colgi stain – highly schematic but showing spatial arrangement: g and h are bipolar cells; i is a horizontal cell; k, r, s, t, and m are amacrine cells; o, p, and q are ganglion cells. This is the off-hand diagram used for illustration in Ramon y Cajal's *Histologic du Systeme Nerveux* (Paris: Maloine, 1909-1911).

2.3 Design of the Model (Ref. 5)

Essentially, the bug detector cell responds to a small dark object which moves centripetally into its responsive field. In the list of the cell's properties given in Table 1, the smallness of the object is item 1b, darkness item 1c, centripetal movement item 1a. Note that the discharge rate of the cell (items 4a to 4g) depends upon the size and location of the object, both measured in degrees or minutes of arc at the lens of the frog's eye. Five minutes of arc are imaged on one photoreceptor.

Table 1. Properties of Bug Detector (Group 2) Ganglion Cell.

1. A Group 2 ganglion cell responds to an object :
 - a. that moves centripetally
 - b. that is small (3° to 5°)
 - c. that is darker than the background
 - d. that has a sharp leading edge
2. There is no response to:
 - a. any object totally outside the responsive retinal field (RRF) of diameter approximately 4°
 - b. a straight edge of a dark band greater than 2° wide unless it is surrounded by a shield approximately 4° in diameter centered on the RRF (Responsive Retinal Field)
3. Response is independent of:
 - a. level of illumination
 - b. rate of change of illumination as long as this is distinguishable
 - c. speed of an edge if it travels between a maximum and a minimum speed
 - d. amount of contrast as long as this is distinguishable
4. Discharge rate is:
 - a. null for dark objects of width less than about $3'$
 - b. inversely proportional to the convexity of an image with diameter greater than $3'$ but less than one half of the angle subtended by the RRF
 - c. maximal (approx. 40 pulses per second) for an image subtending half the angle subtended by the RRF
 - d. proportional to the convexity of images larger than one half of the RRF angle
 - e. feeble if the object is larger than RRF
 - f. greater to movement broken into several steps than to continuous movement
 - g. feeble in response to light spots
5. The response is maintained for several seconds if the object stops in the RRF

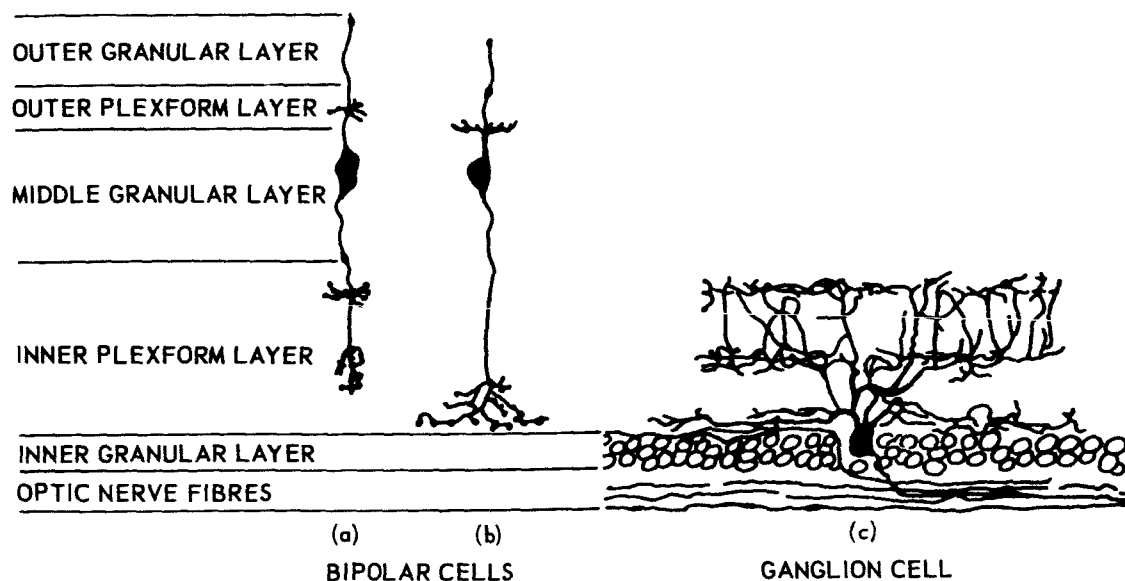


Fig. 3. Retinal sections of two types of bipolar cell and the bug detector ganglion cell in a frog retina (after Ramon y Cajal).

Figure 4 diagrams a model of the bug detector cell designed by Dr. Roberto Moreno-Diaz to meet three conditions. The first was that it fit the experimental data on this type of cell presented in Table 1. The second was that its structure approximate that pictured by Cajal and identified by Lettvin et al. The third was that all of the 1/4 million cells of this type be capable of being built with existing hardware.

Dr. Warren McCulloch feels that in a model of perception, feedback plays an important role. Since this model employs no feedback it cannot be considered an attempt to solve the general problem of perception. It is rather a scheme to match experimental results of physiology with known anatomy, within the restrictions mentioned above.

At the top of Fig. 4, the image of a bug (shaded) is moving toward the center of concentric areas, of radii R_1 and R_2 . The area of radius R_1 (called responsive retinal field or RRF in Table 1) includes approximately 2000 photoreceptor cells, three of which are represented by small cylinders. The larger area represents approximately 20,000 cells; five of which are represented by the three same cylinders and two additional ones.

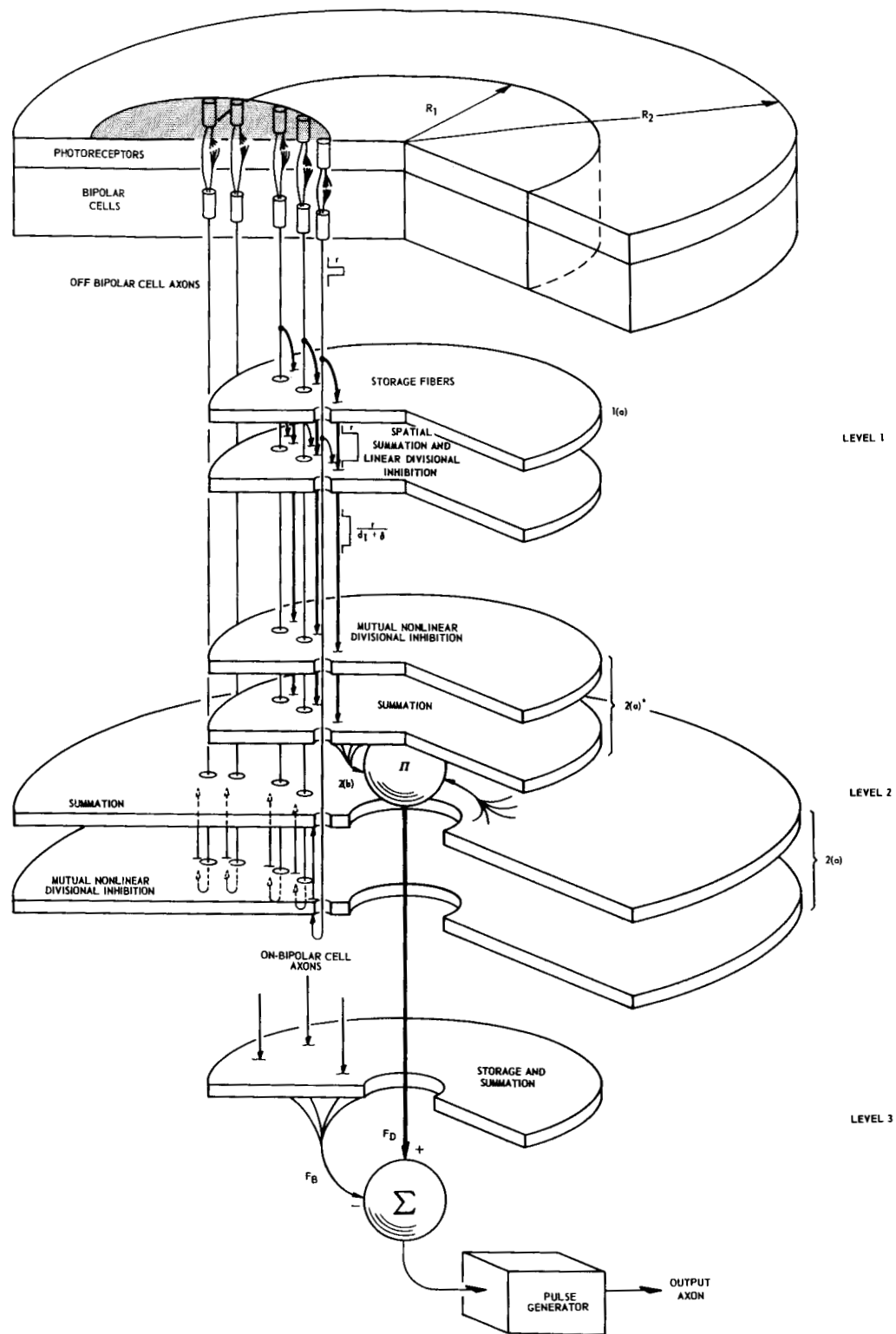


Fig. 4. Diagram of models of photoreceptors, bipolar cells and bug detector ganglion cell.

Between each photoreceptor and bipolar cell are two connections, one fast and one slow. By comparing inputs from these two connections, each bipolar cell determines whether illumination on the retina has increased or decreased. Firing of an off-bipolar cell indicates illumination has decreased, firing of an on-bipolar cell that it has increased. Only off-bipolar cells are shown. On-bipolar cells, whose presence is assumed, connect to level 3.

Levels 1 and 2(a)* of the ganglion cell model respond only to off-bipolar cells in the area of radius R_1 (RRF) to determine the penetration (p) of the bug into this area and the nonlinear response to this penetration. Computations performed in this layer and a half are treated in the following subsection.

Level 2(a) responds to off-bipolar cells in the area of radius R_2 to determine the convexity of the leading edge of the bug. This computation is treated in the second subsection following.

Level 3 responds only to on-bipolar cells in the area of radius R_1 (RRF) to determine, with previous computations, that the motion is centripetal. This computation is described in the third subsection following.

Activity of a bipolar cell is represented by a pulse of amplitude r , as shown in Fig. 4. This pulse is applied through a broad curving branch to level 1(a), through a fine curving branch to level 1(b) and through the lowest slab of level 2(a), to which it returns.

2.4 Computation in Levels 1 and 2(a)*

The pulse of amplitude r that passes through the broad curving branch of the off-bipolar cell axon is stretched in level 1(a), as shown in Fig. 4. While such neural storage usually has an exponential decay, it is here given a square waveform for simplicity. In level 1(b) the amplitude r is divided by the number of photoreceptors in the leading edge of the image, d_1 , plus a constant δ . The second branch — the fine one — makes possible the spatial summation that forms this sum d_1 .

In the first slab of level 2, the advancing pulses interact to inhibit each other in a mutual nonlinear divisional fashion suggested by Schuyperheyn.⁽⁷⁾ The stretched pulses, representing the length of time since

the image moved into the circle of radius R_1 , together indicate the area darkened, D_1 . By the formula for this kind of inhibition,⁽⁵⁾ the amplitude of the signal on the j^{th} wide line in the upper slab of layer 2(a)* is

$$A_j^* = c_1^* \frac{r}{d_1 + \delta} e^{-k_1^* \frac{rD_1}{d_1 + \delta}}$$

The asterisks or stars are applied to the symbols of this layer to distinguish them from the symbols of layer 2(a). The quotient $D_1/(d_1 + \delta)$, which can be approximated D_1/d_1 , is an area divided by the length of the leading edge. It equals approximately the penetration p of this area into the circle of radius R_1 (RRF').

The second slab of level 2(a)* forms a sum A_c^* of all the active A_j^* signals. There are D_1 of these.

$$\begin{aligned} A_c^* &= c_1^* \frac{rD_1}{d_1 + \delta} e^{-k_1^* \frac{rD_1}{d_1 + \delta}} \\ &\approx c_1^* r p e^{-k_1^* r p} \end{aligned}$$

Employing the experimental evidence of Table 1, $k_1^* r$ can be evaluated, leading to

$$A_c^* = c_1^* r p e^{-\frac{p}{0.26R_1}}$$

which is plotted in Fig. 5. The constant c_1^* can be evaluated by a method indicated in Ref. 5.

2.5 Computation in Level 2(a)

The sum of the outputs of the off-bipolar cells, in the area of radius R_2 , in the last time period, is the "length of dimming" d_2 . The signal passed from the lower to the upper slab of layer 2(a) on the j^{th} line is

$$A_j = c_2 r e^{-k_2 d_2 r}$$

where c_2 and k_2 are constants. The interaction represented by this formula is again the "mutual nonlinear divisional inhibition" of J. J. Schypperheyn.

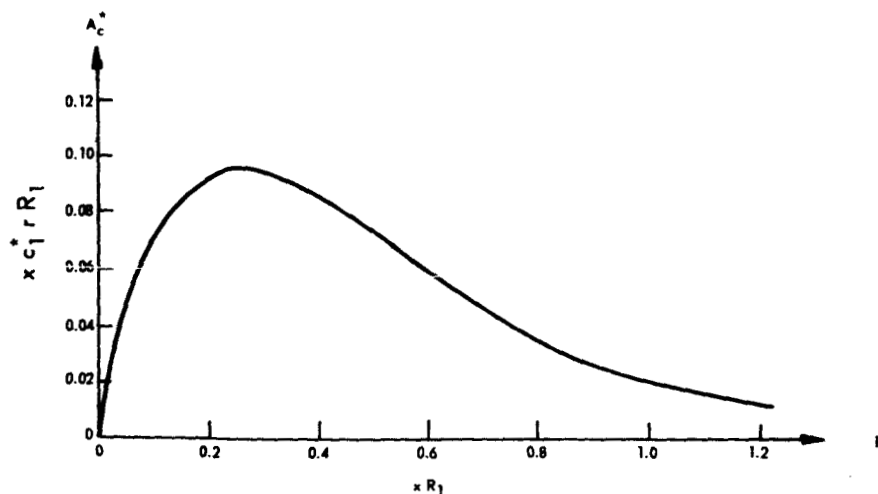


Fig. 5. A_c^* as a function of penetration p .

The upper of the two slabs of layer 2(a) sums the signals on the lines rising from the lower slab and compares the sum to a threshold θ . The sum is represented by A_{net} and can be computed by summing the A_j ,

$$A_c = \sum A_j,$$

and subtracting the threshold

$$A_{\text{net}} = A_c - \theta$$

Figure 6 presents a graph of the sum of the signals, A_c , rising from the lower slab. Figure 7 presents the difference A_{net} . The response is thus made dependent on the size of the object. Experiments on the frog indicate that the smallest object detected is about 3' (Table 1, 4b) of arc wide, that there is an optimum response to objects whose image area is about one half the area of radius R_1 and response falls to zero for objects whose image size is approximately this area, i. e., $d_1 \approx \pi R_1$.

At level 2(b), represented by a sphere, A_{net} , A^* and a constant are multiplied together to yield the function of dimming, F_D :

$$F_D = K_D A_{\text{net}} \cdot A^*$$

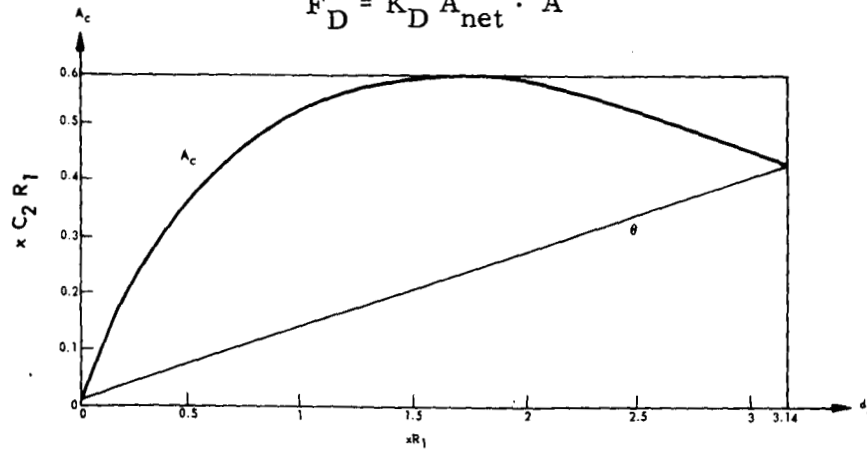


Fig. 6. A_c and θ as functions of the length of dimming d_2 .

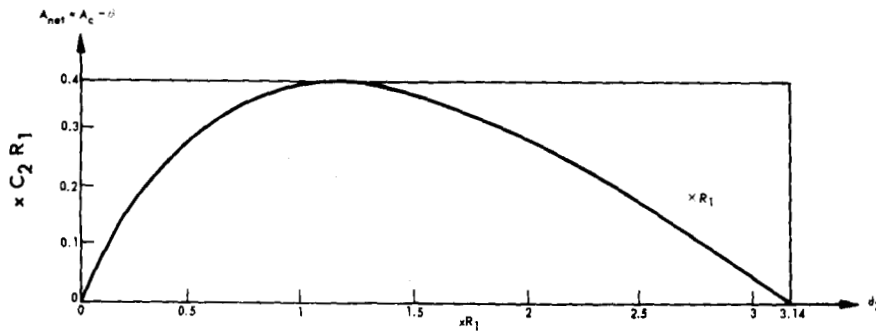


Fig. 7. A_{net} as a function of the length of dimming d_2 .

2.6 Computation in Level 3

The outputs of on-bipolar cells report brightening as the image of the bug advances. Level 3 stretches the pulses from on-bipolar cells, and sums them to give the function of brightening F_B . The summer at the bottom of the diagram takes F_D in a positive sense and F_B in a negative sense to get their difference. The pulse generator emits a frequency proportional to this difference. Thus, only as the dark image of a bug moves toward the center of the field of radius R_1 is there an output. By choice of constants, the pulse rate can be made maximum for an image that subtends half the angle subtended by the area of radius R_1 . This is the condition of maximum response of the living cell.

2.7 Instrumentation with Available Components

Using elements of previous designs of models of frog retinas,⁽⁴⁾ Dr. Moreno-Diaz devised the hardware model shown in Fig. 8. To permit placing the entire design on one page, we have shortened each vidicon into a wide flat bottle.

The two vidicons at the top view the same scene through a beam splitter. The raster of each tube comprises 500×500 or $1/4$ million positions. If this resolution is maintained through the model approximately $1/4$ million bug detector ganglion cells will be represented.

The bipolar cells are represented by the summer (Σ) and diodes that follow it. If the output of the summer is negative, representing dimming, the output goes to the cathode ray tube and vidicon combination immediately below it. If the output is positive, representing brightening, it goes to the CRT-vidicon in the lower part of the illustration.

The model of the bug detector ganglion cell is divided into three levels as in Fig. 4. In level 1 of Fig. 8, dimming is mapped on the face of the cathode ray tube. Fibre optics communicate the slowly fading image to a vidicon. The combination of tubes, commercially available as a scan conversion tube, performs temporal summation.

The output of the vidicon goes to a pulse generator (PG) which delivers its output to a bank of shift registers which map 50 lines of the vidicon raster. Attached to the shift registers and representative of the area of radius R_1 in Fig. 4 is a summer (Σ) which determines the part of the area of radius R_1 that has been dimmed, D_1 . The bank of shift registers work this way: As the first position of the first line of the raster is scanned, a 1 or 0 is fed to the first shift register. As successive positions are scanned, successive 1's or 0's are fed to the first shift register. At the start of the second line of the vidicon raster, the 1's and 0's in the first shift register are fed to the left end of the second shift register. After 50 lines have been scanned 1's and 0's representing the dimming in these lines will be loaded in the bank of 50 shift registers. From then on the registers overflow but always contain 50 lines.

The length of dimming d_1 is computed in the second bank of shift registers and combined with D_1 in the box labelled \div . The quotient D_1/d_1 is the

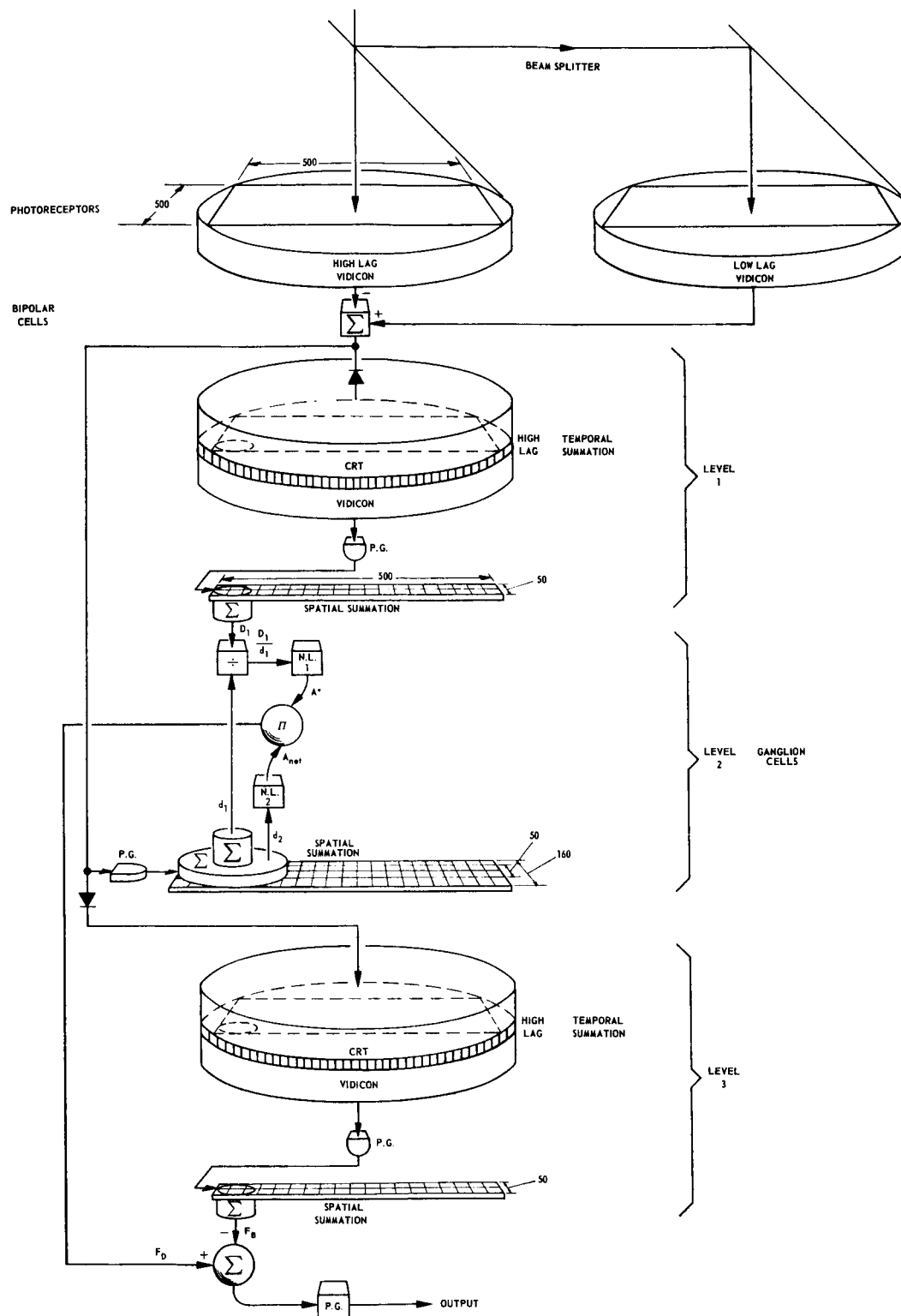


Fig. 8. Possible instrumentation of 1/4 million Moreno-Diaz models of the bug detector ganglion cell.

penetration p of the image of the bug into the area of radius R_1 . The box labelled "N. L. 1" performs the nonlinear transformation of Fig. 5.

The second shift register and its large-area summer (Σ) computes the length of dimming d_2 . This is fed to Nonlinear Circuit 2 which performs according to Fig. 7. The analog multiplier labelled π combines A_{net} , A^* and a constant to form F_D .

In level 3 a second combination of cathode ray tube and vidicon determine the areas brightened in the whole retina. A third bank of shift registers and summer determine the brightened area B_1 for each cell. F_B is proportional to B_1 . The final summer subtracts F_B from F_D . The final pulse generator yields a pulse frequency proportional to this difference.

2.8 Instrumentation with Integrated Circuits

We are now redesigning the system of Fig. 8 to employ integrated circuit elements instead of vidicons and cathode ray tubes. Figure 9 shows an array of 50×50 photo transistors developed by Westinghouse.⁽¹⁰⁾ That company has since built four times as many units in the same area.

We are on the way, we think, of devising a way of using this kind of array. From our point of view, it has two difficulties. One is the difference in response characteristics between phototransistors. The other is defects in phototransistors, i. e., some may not function at all. In a system we are designing the output of each phototransistor will be compared to its own previous output. Thus discrepancies between phototransistors should not enter the computation.

2.9 Application to a Mission to Mars

Design of a layered processor to recognize a bug of a particular size and travelling in a particular direction indicates that other recognition systems can be designed both to recognize predetermined objects and objects newly experienced. Such recognition is a reduction in data, because it permits reporting simply the presence of the objects. The system about to be described should also permit reporting the location of an object.

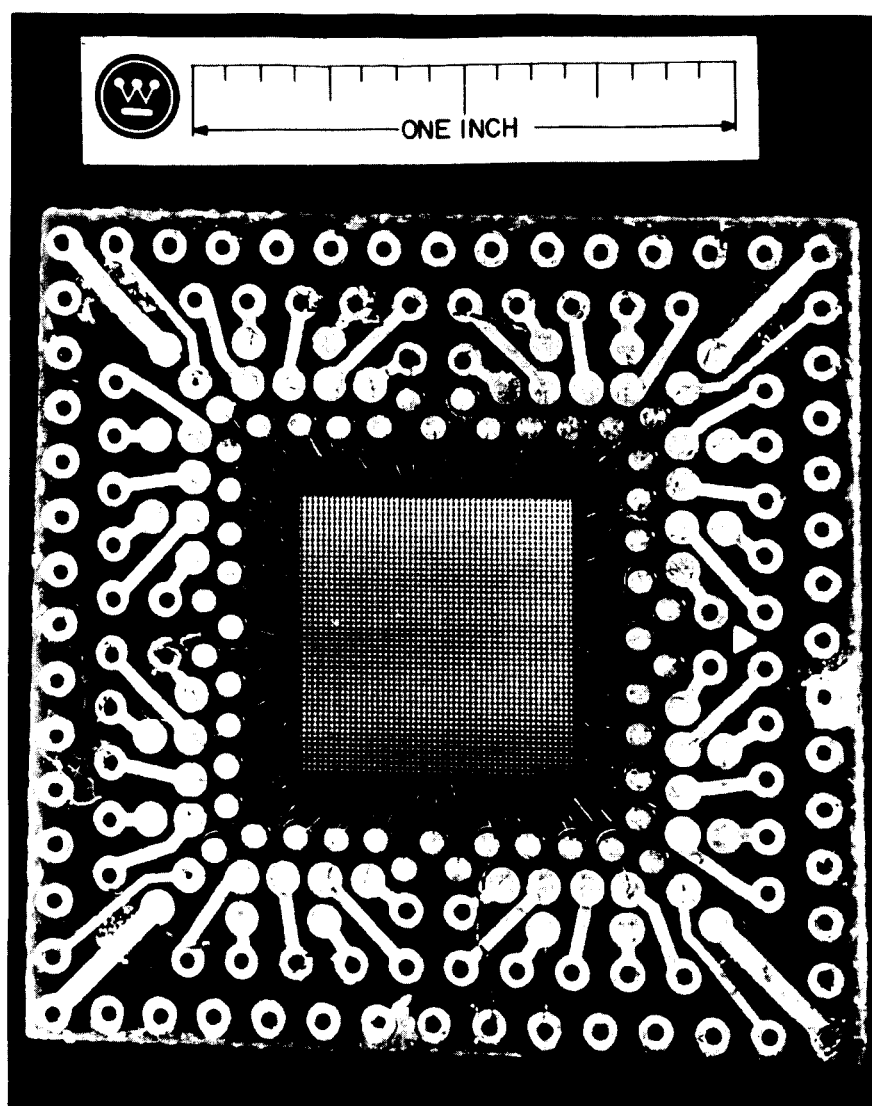


Fig. 9. Array of 50×50 phototransistors developed by Westinghouse.

3. STEREOSCOPIC SYSTEMS

3.1 Why Stereoscopic?

One of the tasks a robot may have to perform is to discover separate objects so as to avoid them, if moving, or describe them in detail if they have properties of interest. Several strategies are possible in the use of a pair of television cameras coupled to a computer. One that we are considering is diagrammed in Fig. 10.

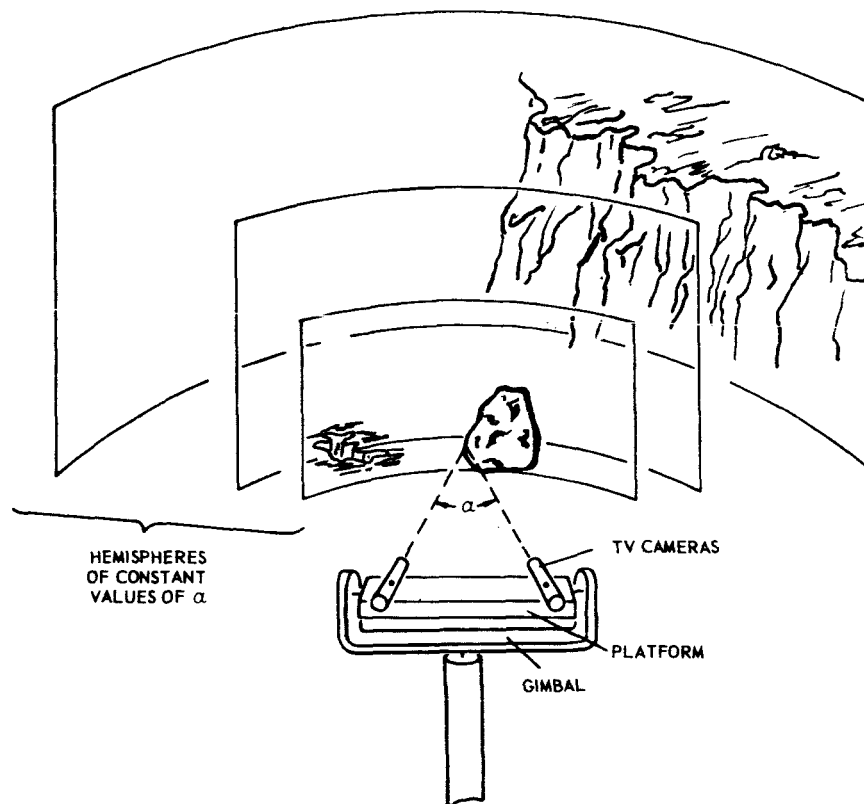


Fig. 10. A strategy to discriminate objects by a stereoscopic pair of TV cameras and a computer.

Here the cameras have mechanically scanned the innermost of three hemispheres until they have encountered the edge of a rock. The hemisphere scanned is that for which the angle of convergence of the two cameras is the value of the angle α shown. For a smaller value of α , the hole could be encountered. For a still smaller value, the edge of the cliff could be encountered. The problem is how to bring about the encounter.

3.2 Camera-Counter Chain C

To carry out initial experiments, we have attached a beam splitter to the front of a television camera, as shown in the illustration of our Model C camera computer chain (Fig. 11). The geometry of the two views is shown in Fig. 12. The prism of the previous illustration is here omitted for simplicity and the single camera shown as two. The left camera looks out through the lower cone, the right through the

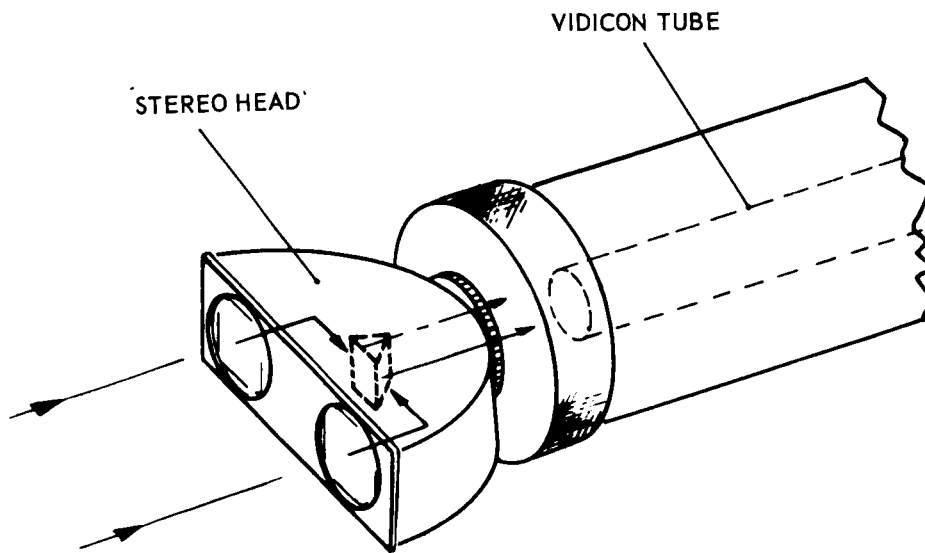


Fig. 11. Front end of Model C camera computer chain.

upper cone, the two cones overlapping some distance in front of the cameras. The point P on the edge of the right cone is near the center of the lower cone. It is imaged at P'_R on the right half of the camera, at P'_L on the left half of the camera.

Left and right TV frames have been drawn in front of the cameras to illustrate the method of computation. To search for an object such as that with the angle of convergence α shown in Fig. 11, windows will be advanced from left to right across the frames. Computation then can be limited, at any instant, to interpretation of the data in the two windows.

3.3 Camera-Computer Chain D

A constraint on camera-computer chain C is that it employ a lens of average focal length. Thus each camera sees neither a full field of view nor the narrow field of view that provides high resolution. To obviate this difficulty, camera computer chain D is being designed. (See Fig. 13.) It has interchangeable lenses and each camera is mounted to swivel. In addition, the cameras are mounted on a platform that nods.

Figure 14 shows a possible configuration of cameras and computers to visually explore a scene and report, according to the strategy described

above, first the presence of free-standing objects then details about one or a few of these objects.

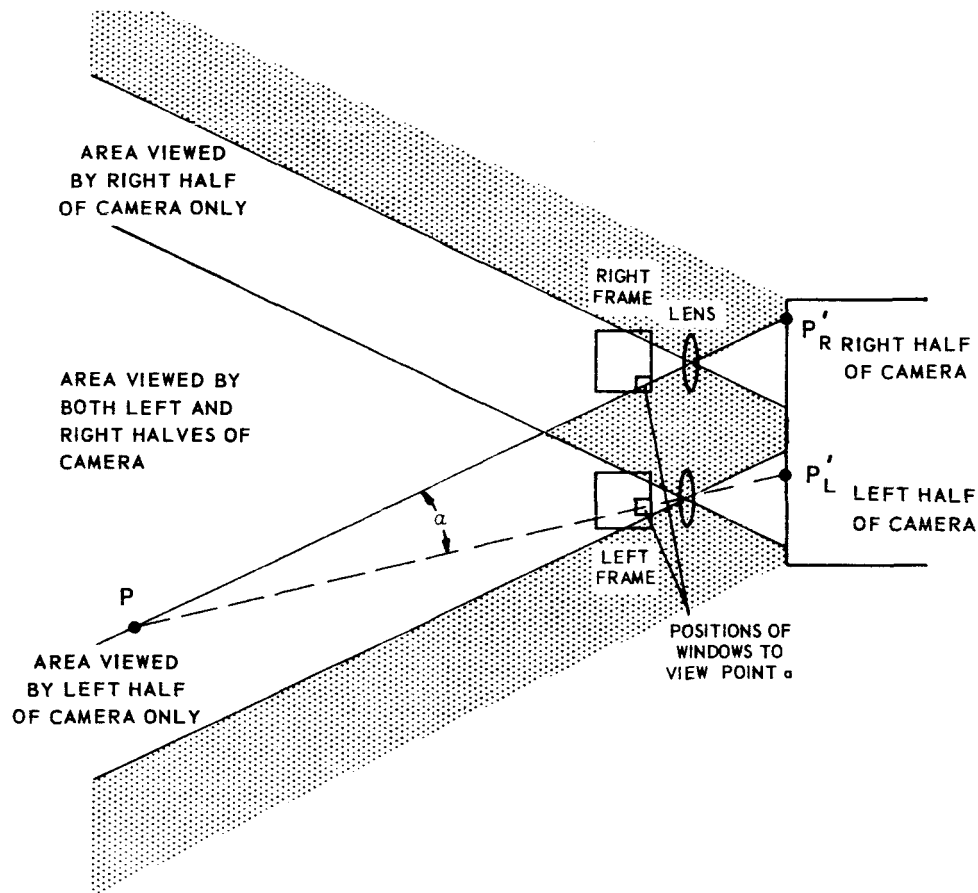


Fig. 12. Schematic of front end of Model C camera computer chain.

3.4 Application to Missions to Mars

If several free-standing objects are detected, how is one to be selected for more detailed examination? An animal could use another sense, such as the sense of touch. We are planning senses other than that of vision. In the following section we refer to these as sense modalities. The problem then arises: How should a robot combine the inputs from different sense modalities to decide what to do?

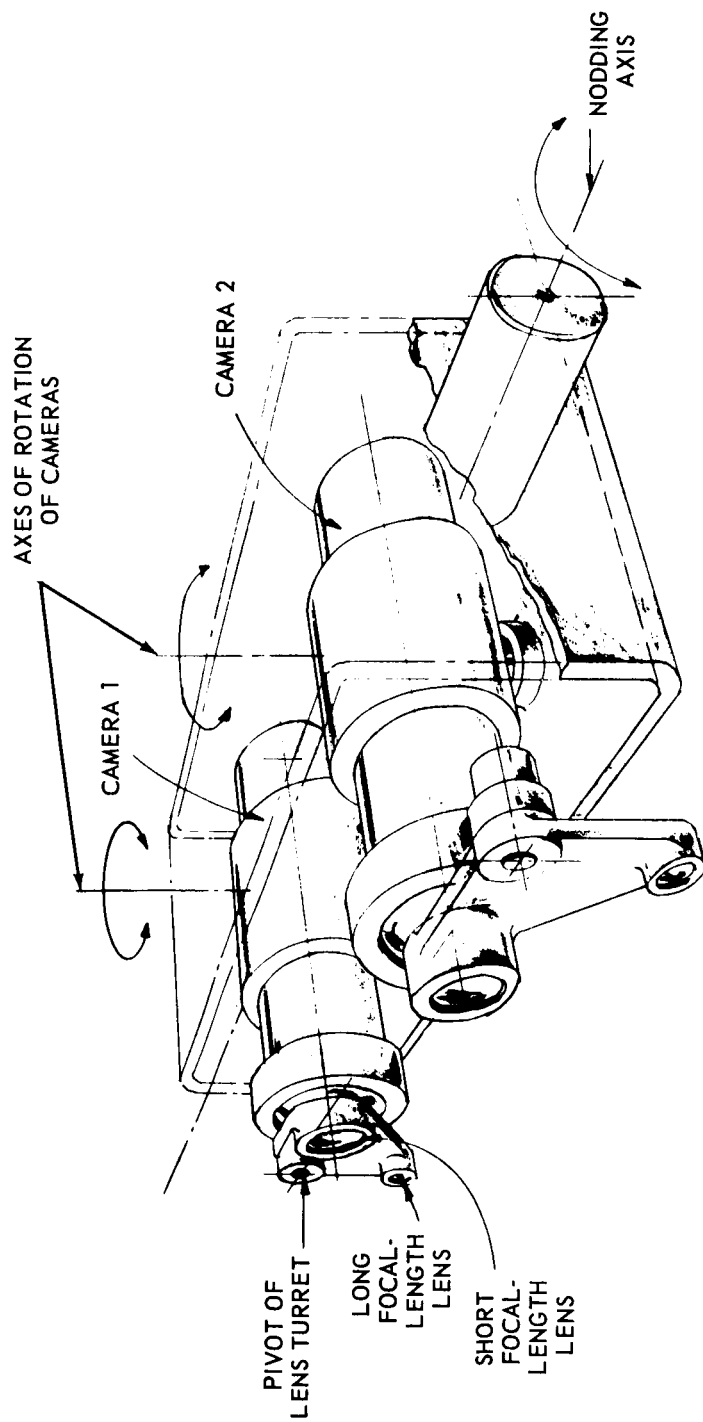


Fig. 13. Front end of Model D camera computer chain.

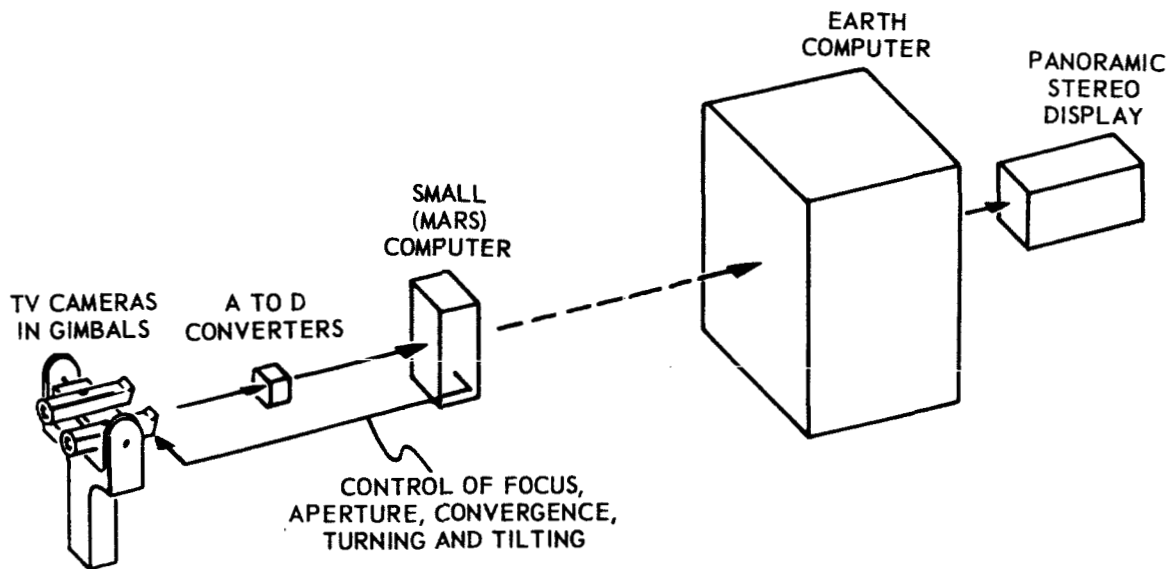


Fig. 14. Block diagram of Mars-Earth camera computer chain.

4. DECISION AND CONTROL PROCESSORS

4.1 General

As we enter into the field of layered processing of information we are in strange territory. There is no mathematical theory of nonlinear integral transforms. There is no theory for handling purely informational (as opposed to power) feedback. Group theory is concerned with better defined cases than what we are handling.

But, if layered computation seems the method used by all brains, it may be one of the necessary conditions for doing what an animal does. There is no way by which sequential operations map parallel operations if the elements in a layer are also mutually connected, as seems the case in most of brain. Thus we have had no recourse but to start simulating and trying before we adduce general design principles.

Two ventures in computer design beside the design of eyes will now be presented. First is the model of reticular formation designed by Drs. McCulloch and Kilmer.⁽¹¹⁾ Second is a processor for the output of our "eye" (described under "Visual Center" below).

4.2 Reticular Formation

The reticular formation (RF) integrates the sensory-motor and autonomic-nervous relations so as to permit an organism to function as a unit instead

of a mere collection of organs. The core of all nervous systems, it extends throughout the length of the spinal cord and into the cranium. (See Fig. 15.) It receives inputs from all of the separate sensory systems, auditory, visual, olfactory, vestibular, etc., and from all of the housekeeping systems involving visceral regulation, respiration, cardiovascular control, etc. Figure 16 shows the wide flat spread of the reticular cells to which the inputs connect and between which the reticular cells interconnect.

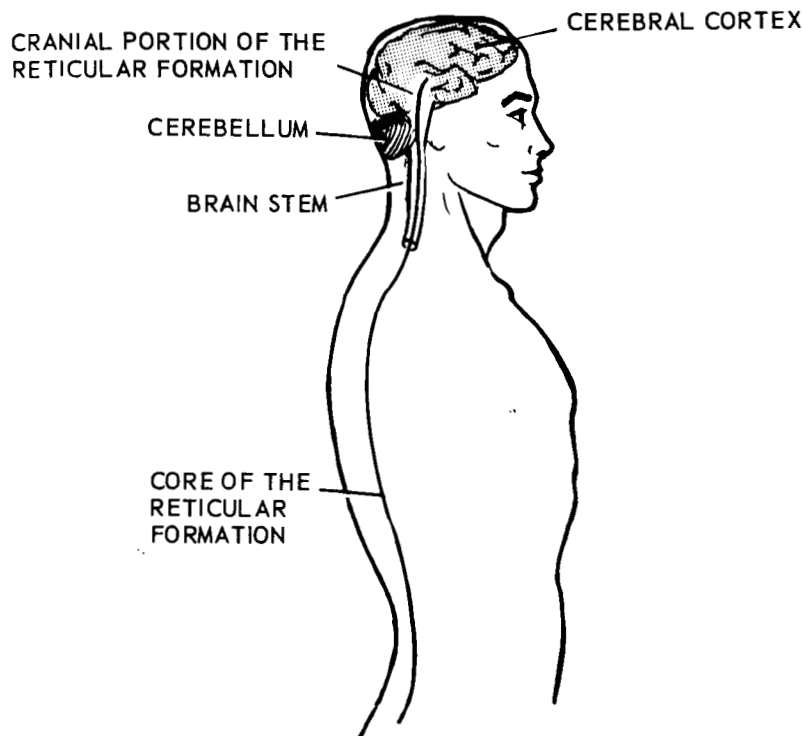


Fig. 15. Core of the reticular formation in the cranium, brain stem and spinal cord of man.

As Kilmer et al⁽¹²⁾ say, "The Scheibels⁽¹³⁾ have so far done the most definitive neuroanatomy that we have on the reticular formation. In their milestone report of 1962 they caricatured its anatomical structure in the brain stem by comparing it to a stack of poker chips. In each chip region the dendritic processes of RF neurons ramify in the plane of the chip face, often covering nearly half of the face area. This causes a very large degree of overlap and intermingling among dendrites of

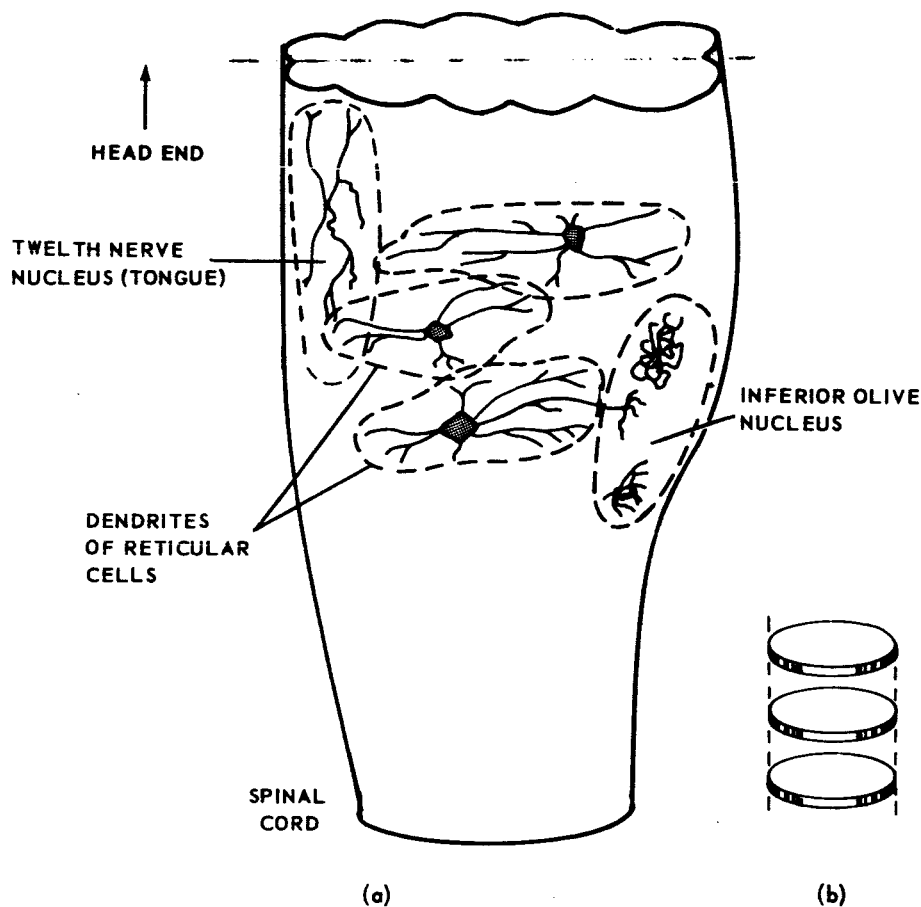
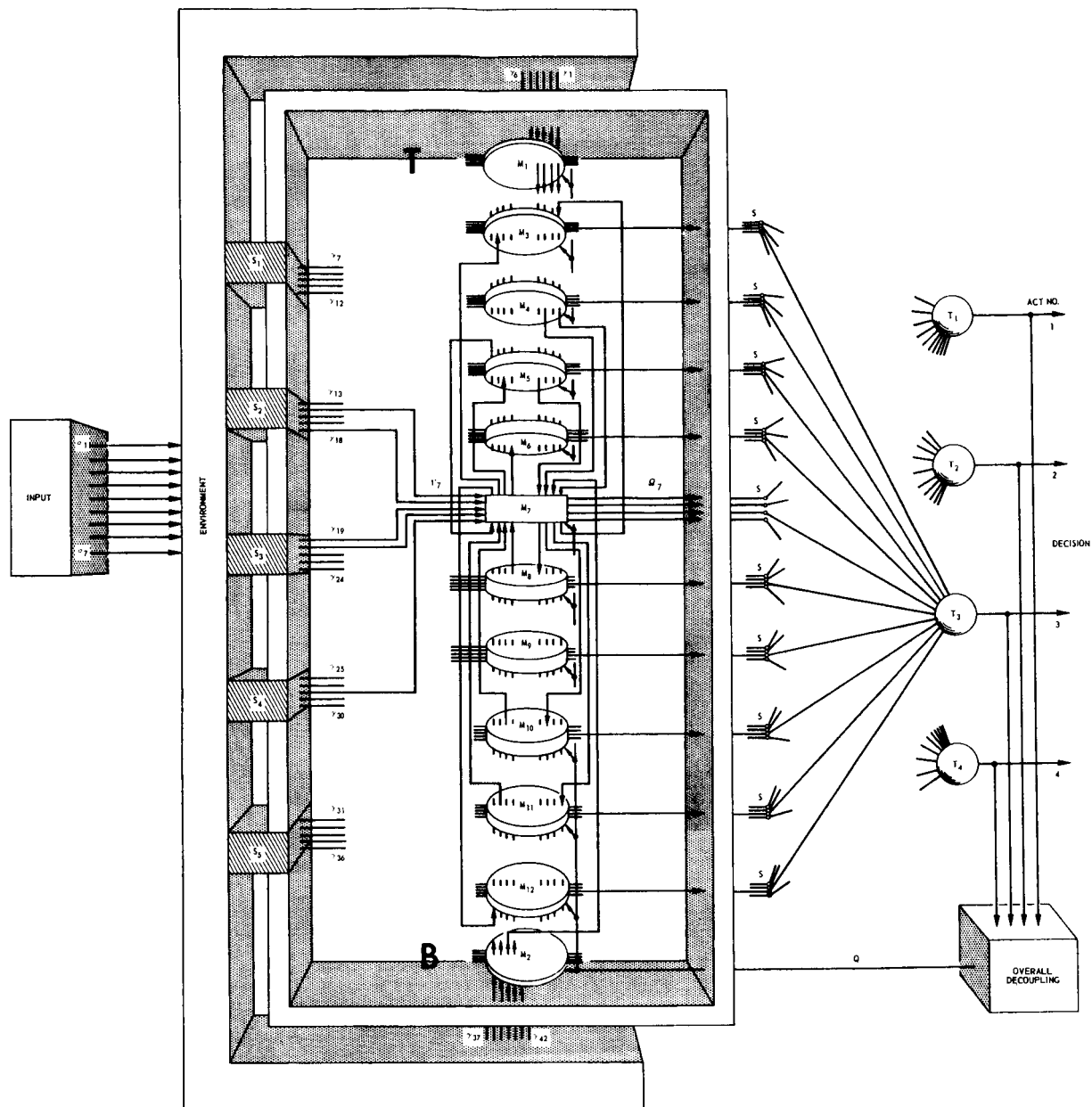


Fig. 16. (a) Dendritic ramifications from three cell bodies in the reticular formation, from two in the inferior olive and from one in the twelfth nerve nucleus (kitten brain, Scheibel, 1962)

(b) Poker chip caricature of reticular cell dendritic ramifications in (a)

nearby neurons, as shown schematically for just the brain stem region in Fig. 16. (This is very similar to Scheibels' Figure 1 in reference 13.) . . . Since as many as half dozen or more input systems may synapse on a single RF neuron, and each RF input nucleus and fibre tract in general feeds very many RF cross-sectional levels, the Scheibels suggest that the RF might tolerate considerable puddling of information at each of its cross-sectional levels, but demand somewhat



Legend (from left to right)

σ_i	factor of the environment	M_i	module i
S_i	sense	Ω_i	four components of the probability vector from module i
γ_i	input	s	step function
Γ_i	inputs to module i	T_i	threshold element

Fig. 17. Schematic of the computer-simulated RF*.

greater informational rigor between levels. Figure 16(b) is a caricature of the dendritic fields, comparing them to a stack of poker chips.

"In its non-specific control of sensory inputs, the reticular formation is analogous to an admiral-of-the-fleet, committing the organization under its command to one act, trusting that fine perceptions are made at their centers of specialty and are accurate. As a computer, the reticular formation is seen to be broad in its domain of command but exceedingly shallow in any specific area under its command. It commits the organism to an act which is a function of the information that has been played upon it in the last fraction of a second or so. After commanding the organism to act, e. g., fight, run, swallow, vomit, sleep, copulate, etc., it sends out control directives to all of the specialized centers of the central nervous system, tuning their activities to this task.

"Its important features are that it must handle a vast amount of highly correlated input information and arrive at one of a small number of mutually exclusive acts in a dozen time steps or so and with minimal equipment. The crucial information as to what act the organism has selected is distributed over its input lines.

"In this paper we are concerned only with that part of the RF which makes the decision to commit the organism, henceforth denoted RF*. RF* is RF minus everything on the RF's input side (the dorsal-lateral RF) and output side (the ventral-lateral RF, basal ganglia, etc.), all of the reflexes along the neuraxis that are handled locally, and all of the respiratory and other rhythmic operational aspects which are functionally separable from the decisionary task." (RF* is called \overline{RF} in Ref. 11.)

4.3 Model of RF*

"Figure 17 shows a schematic of a decision and control model analogous to the reticular formation. Each of the modules in the figure is a hybrid computer of the type shown in Fig. 18. The 42 input lines, γ_i , to the modules in Fig. 17 are connected in a several-to-all, but not all-to-all, fashion to the modules. The top of the

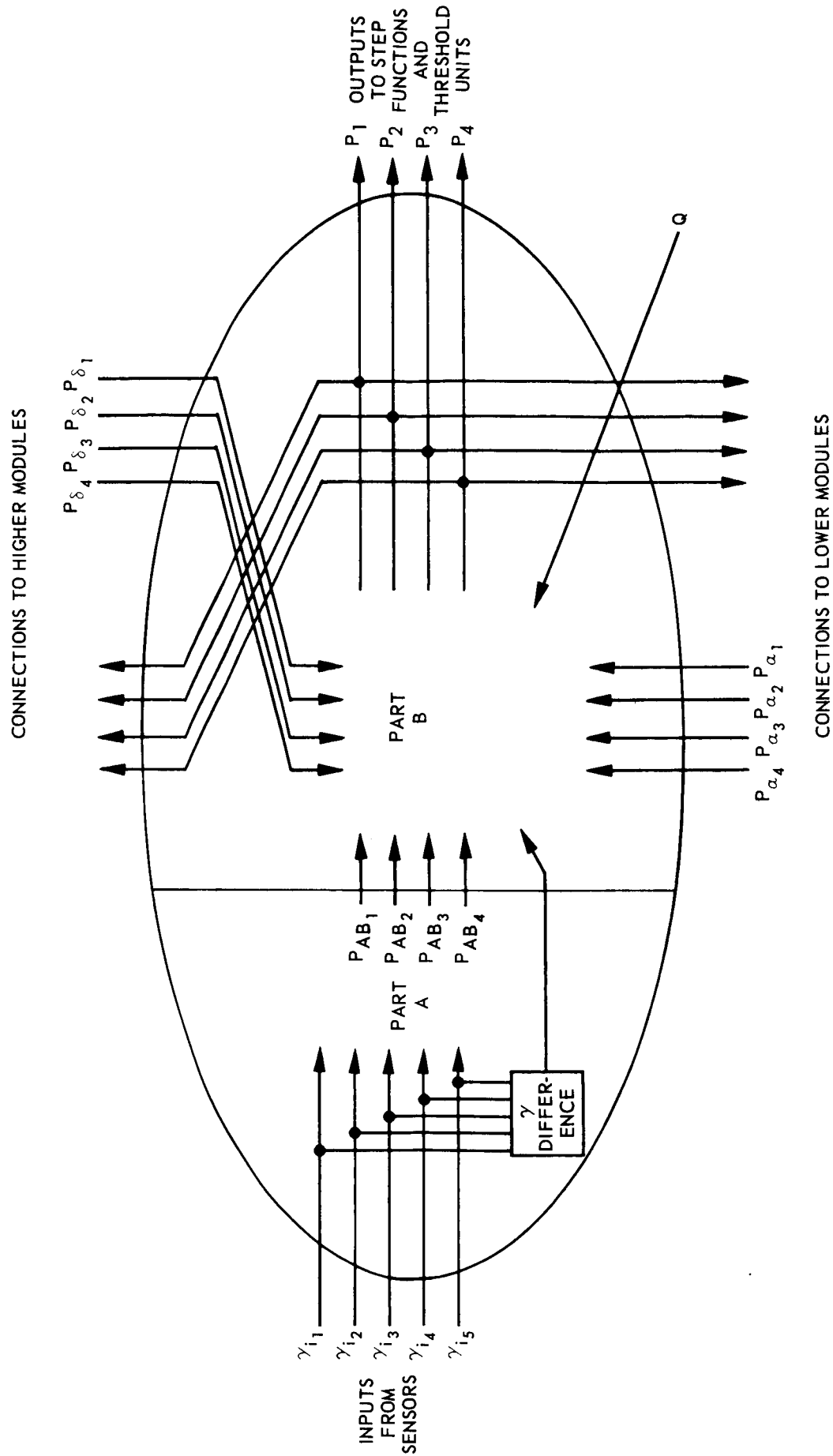


Fig. 18. Input and output connections to parts A and B of a module.

drawing (T) and the bottom (B) correspond roughly to the diencephalic and high cervical regions, respectively, of higher vertebrates. The white-boundaried half-box represents the environment of the organism being modelled. The environment is established by factors, σ_i , of the set Σ . The S_i represent exteroceptive, interoceptive, and internuncial systems which sense this environment and feed highly (but nontrivially) correlated inputs, γ_i , directly into the model. For convenience, all σ_i and γ_i lines are binary.

"There are twelve logic modules in the simulated RF*. The sets of lines \mathcal{Q}_i (only \mathcal{Q}_7 is marked) indicate the act preferred by module M_i . There are four lines in each set because the model is at present capable of four acts. The four lines carry the four components of a probability vector.

"For clarity, all types of connection lines (Γ, \mathcal{Q} , ascending and descending lines) are shown only for module M_7 , whereas these types of connection are actually made to all regular modules. Each M_i receives inputs from several but not all S_j , and each S_j feeds several but not all M_i .

"Each module (Fig. 18) computes directly on the input information that it receives and makes a best guess as to what the corresponding act should probably be. After the initial guess, the modules communicate their decisions to each other over low capacity information channels. Then each module takes the information (from all other modules) and combines it in a nonlinear fashion with the information coming directly into it to arrive at a mixed guess as to what act should be performed. This is in turn communicated to the subset of modules to which it is connected above and below. Thus we have decomposed the module shown in Fig. 18 into two parts. The A part operates on the module's input information. The B part operates on information from above, below and from the A part.

"The A part with five binary input variables and four analog output variable outputs, is a nonlinear probability transformation network."

Quoting Ref. 14, "The B part receives 4-component probability vectors P_δ from the above, P_α from below and P_{AB} from the A part. The j^{th} component of each probability vector is the probability, computed by the module of origin, that model RF*'s present γ input signal configuration demands act number j . The B part also receives the difference between γ inputs, called " γ difference" in Fig. 18, and the overall decoupling Q shown being formed in Fig. 17. The B part yields the module's determination of the probability that the model RF*'s present γ input signal configuration demands act number j .

"The design of the modules was straightforward. The main problems concerned the way in which the computation converged to produce consensus. This consensus is achieved, as illustrated in Fig. 17, by first determining at point s if the j^{th} component of the probability vector P from each module exceeds 0.5. If it does, a 1 is passed on to the threshold element T . There, if 60% of the input connections are 1's, act j is decided upon. Note that each element T in Fig. 17 receives 10 inputs. For clarity of the drawing connections are shown only to T_3 . The threshold elements T are crude models of the muscle systems of animal which receive many inputs, decode them and act.

"The model has been successfully simulated on the M. I. T. Instrumentation Laboratory Honeywell Computer in collaboration with Jay Blum, E. Craighill and D. Peterson. The model converged to the correct act in each of about 50 test cases, and always in from 5 to 25 time steps.

"We are now concentrating on the functional design of a considerably enriched model which can handle conditioning and extinction in a satisfactory time domain sense."

4.5 Visual-Center

Walter Pitts once pointed out the consequences of having sequences of widely connected layers such as exist in a brain. It is that there will exist "stimulus" equivalences in the output — and the classing of stimuli

into "similar" and "dissimilar" may not necessarily follow those which would be natural to us. Nor could we from analyzing the connectivities in the net determine what these classifications would be.

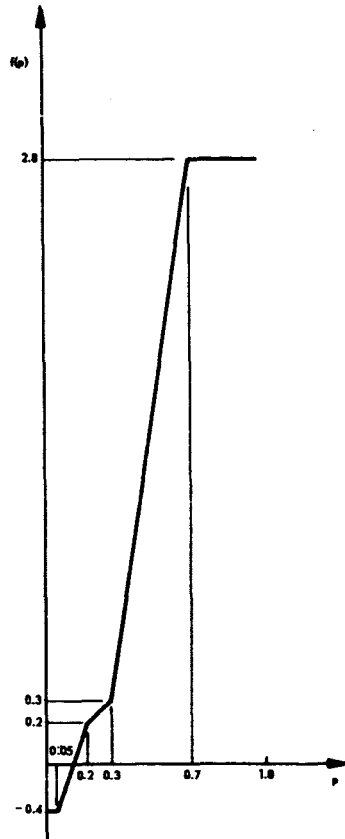


Fig. 19. The $f(p)$ function.

We intend, however, to superpose on our "eye" other layered nets so as to come, by patch and try, to a kind of excerpting of forms from the image as classes in the output. We have no idea yet of our chances for success. But the method must be tried.

4.6 Application of RF* to Missions to Mars

As Dr. Kilmer puts it, ⁽¹⁵⁾ "Our next task will be to sufficiently enrich the present model of RF* to enable it to exhibit several types of learning. This will require the insertion of delay chains between modules and the addition of adjustable decision circuitry in the a part of each module."

A task beyond this will be to tie the visual center to the model of RF* through far more channels than are shown in Fig. 17. Other sense modalities will be needed such as the sense of touch. Dr. Kilmer suggests that on Mars the model of RF* may have to decide among the following acts:

1. Rest
2. Locomote to _____
3. Turn around
4. Preprogrammed operation mode I
5. Preprogrammed operation mode II
6. Preprogrammed operation mode III
7. Maintenance
8. Communication to space vehicle (landed) I
9. Communication to space vehicle (landed) II
10. Righting (after overturn)

For example, if operation mode I were a visual experiment, it would not be switched on in darkness or a very high wind. For another example, if operation mode II were a soil assay experiment, only conditions of warmth and low wind velocities might trigger it.

5. THE NEED TO CARRY KNOWLEDGE ALONG

To be useful, such a device has to know something, as Lettvin, Maturana, Pitts, and McCulloch concluded when they started to study a frog's eye. What a frog knows in its retina is described above.

To look for what scientists need to learn about the surface of Mars, our device must know what the scientists are looking for. We shall be happy to respect their wishes.

LIST OF REFERENCES

1. Lettvin, J. Y. , Maturana, H. R. , McCulloch, W. S. , and Pitts, W. H. , What the Frog's Eye Tells the Frog's Brain, Proc. of the IRE, p. 1940, November 1959.
2. Maturana, H. R. , Lettvin, J. Y. , McCulloch, W. S. , and Pitts, W. H. , Anatomy and Physiology of Vision in the Frog (Rana Pipiens), Journal of General Physiology, pp. 129-175, July 1960.
3. Lettvin, J. Y. , Maturana, H. R. , Pitts, W. H. , and McCulloch, W. S. , Two Remarks on the Visual System of the Frog, Sensory Communication, W. Rosenblith, ed. , pp. 757-776, 1961.
4. Sutro, L. L. , editor, Advanced Sensor and Control System Studies, 1964 to October 1965, R-519, Instrumentation Laboratory, Massachusetts Institute of Technology, Cambridge, Massachusetts, p. 16, January 1966.
5. Moreno-Diaz, R. , An Analytical Model of the Group 2 Ganglion Cell in the Frog's Retina, E-1858, Instrumentation Laboratory, Massachusetts Institute of Technology, Cambridge, Massachusetts, October 1965.
6. Ramon y Cajal, S. , Die Retina der Wirbelthiere, Tafel II, Fig. 6 Wiesbaden, Verlag von J. F. Bergmann, 1894.
7. Schwyperheyn, J. J. , Contrast Detection in Frog's Retina, Acta Physiol. Pharmacol. Neerlandica 13, pp. 231-277, 1965.
8. Hartline, H. K. , The Response of Single Optic Nerve Fibres of the Vertebrate Eye to Illumination of the Retina, Amer. J. Physiol. , Vol. 121, pp. 400-415, February 1938.
9. Sutro, L. L. , editor, op. cit. , pp. 10-38.
10. Westinghouse Electric Corporation Aerospace Division, Baltimore, Md. , Advanced Molecular Systems Technology, Volume 1 Systems Applications, pp. 4-11 to 4-16, November 1964.
11. Sutro, L. L. , editor, op. cit. , pp. 84-95.

12. Kilmer, W. L. , McCulloch, W. S. , and Blum, J. , Towards a Theory of the Reticular Formation, 1966 IEEE National Convention, Cybernetics Session, March 14, 1966, New York City, New York, as modified for this paper.
13. Scheibel, M. and A. , On Neural Mechanisms for Self-Knowledge and Command, Mitre Report SS-3, First Congress on the Information Sciences, Mitre Corporation, Bedford, Massachusetts, 1962.
14. Kilmer, W. L. , Summary of Research Progress, Research Laboratory of Electronics Quarterly Progress Report, July 15, 1966, as modified for this paper.
15. Kilmer, W. L. , Section in Advanced Sensor and Control System Studies, April to June 1966, R-548, Louis Sutro, Editor, Instrumentation Laboratory, Massachusetts Institute of Technology, Cambridge, Massachusetts, (in preparation).